

# Tunable diffractive optical elements for hard x-rays

Christian David\*<sup>a</sup>, Bernd Nöhammer<sup>a</sup>, Eric Ziegler<sup>b</sup>, Olivier Hignette<sup>b</sup>

<sup>a</sup>Laboratory for Micro- and Nanotechnology, Paul Scherrer Institute, Switzerland

<sup>b</sup>European Synchrotron Radiation Facility, Grenoble, France

## ABSTRACT

We describe the fabrication and testing of a novel type of tunable transmission hard x-ray optics. The diffractive elements are generated by electron beam lithography and chemical wet etching of <110> oriented silicon substrates. Structures with widths down to 100 nm and extreme aspect ratios were obtained using this method. By tilting the lenses with respect to the x-ray beam, the effective path through the phase shifting structures can be varied. This makes it possible to optimize the diffraction efficiency for a wide range of photon energies, and to obtain effective aspect ratios not accessible with untilted optics. The diffraction efficiency of a Fresnel lens was measured for various energies between 8 keV and 29 keV. Values close to the theoretical limit (approx. 35%) were obtained.

The described technique provides focusing in one direction only. For two-dimensional focusing, two linear lenses with different focal lengths and orthogonal orientations can be placed along the optical axis. Depending on the coherence properties of the source, such an arrangement can improve the resolution and flux compared to a single circular zone plate.

The wet etching technique is also applied to the fabrication of linear gratings with pseudo-random pitch, which will be used as one-dimensional decoherers to adapt the coherence of a synchrotron beam in a defined way. Linear gratings with uniform line density can be used as beam splitters for applications such as holography or interferometry.

Keywords: Zone plate, coherence, decoherer, beam splitter, interferometry, electron-beam lithography, wet etching

## INTRODUCTION

The availability of modern 3<sup>rd</sup> generation synchrotron sources with high flux and high degree of coherence has created a big demand for adequate optical components. For example, the focusing of hard x-rays ( $h\nu > 8$  keV) to sub-micrometer dimensions is an important prerequisite for many techniques such as microanalysis, microscopy, microspectroscopy, and microdiffraction. Reflective, grazing incidence optics are most commonly used for this purpose, but sub-micron spot sizes can only be obtained currently with great difficulty due to aberrations stemming from imperfections of the mirror surfaces<sup>1</sup>. Furthermore, high quality focusing mirror systems are difficult to align and expensive. Due to their complexity, they are usually integral components of synchrotron beam lines, which limits their flexibility.

The first devices to achieve sub-micron hard x-ray focusing in a routine fashion were Bragg-Fresnel lenses (BFLs)<sup>2</sup>. These devices usually consist of a Bragg crystal patterned with a diffractive Fresnel lens. Although BFLs with zone widths down to 100 nm and good diffraction efficiency have been made<sup>3</sup>, there are some severe difficulties in their practical application. This is due to the fact that the optical axis of the setup has to make a large additional angle, which - in contrast to mirror optics - changes with the photon energy. Therefore, BFLs are used in very few experimental set-ups. Focusing transmission lenses avoiding these difficulties would be most useful in a wide range of applications.

Some years ago it was recognized that compound refractive lenses (CRLs) might provide an alternative way to focus hard x-rays. CRLs were first proposed and patented by T. Tomie<sup>4</sup> and shortly later experimentally verified by A. Snigirev et al.<sup>5</sup> Two alternative arrangements are presently in use. The first type consists of a linear array of holes along the optical axis drilled into a block of low absorbing material, preferentially *Be*. The cylindrical shape of the refracting surfaces leads to inevitable spherical aberrations, which limit the obtainable spot size to some microns. The second type consists of low absorbing disks stacked along the optical axis with the refractive shape embossed into the surfaces of each disk. This method allows to avoid spherical aberrations by using parabolic surfaces, and sub-micron focusing has been demonstrated using *Al* as the lens material. However, for acceptable focal lengths the high absorption of *Al* limits the transmission of these devices to about one percent<sup>6</sup>. The fabrication of aspherical refractive lenses from *Be* with adequate quality has not been possible yet due to the hardness and brittleness of this material.

\* christian.david@psi.ch; phone +41 (0) 56 310 3753; fax +41 (0) 56 310 2646; <http://www.psi.ch/lmn>; Laboratory for Micro- and Nanotechnology, Paul Scherrer Institute, CH 5232 Villigen-PSI, Switzerland

Diffraction transmission lenses (Fresnel zone plates) have been used successfully for x-ray focusing and imaging. Spot sizes in the range of tens of nanometers for soft x-rays<sup>7-11</sup> and of about 100 nm for hard x-rays<sup>12</sup> have been achieved. The diffractive patterns are mostly generated by electron beam lithography. State-of-the-art lithography tools are capable of positioning the diffractive structures with accuracies in the order of several nanometers. As the required zone placement accuracy for avoiding aberrations is in the order of the outermost zone width, the resolving power of a zone plate fabricated with state-of-the-art e-beam tools is diffraction limited. Thus, the obtainable spot size is approximately equal to the width of the outermost zones when the lens is irradiated with spatially coherent light. This means, that in contrast to refractive or reflective hard x-ray optics, the coherence of the incoming light is preserved. This feature becomes increasingly important in experiments taking advantage of the high coherence provided by modern synchrotron sources<sup>13</sup>.

The efficiency of a zone plate, as of any other diffractive optical element, depends on the phase shift and attenuation caused by the diffracting structures. For a given photon energy and material, the maximum obtainable efficiency and the necessary structure height to obtain this value can be calculated using scalar diffraction theory<sup>14</sup> and the optical constants tabulated by Henke et al.<sup>15</sup>. The maximum first order diffraction efficiency and optimum structure height for a selection of materials is depicted in Figure 1 as a function of photon energy. Even for high photon energies ( $h\nu > 8\text{keV}$ ), medium weight (Ni, Ge) and heavy materials (Ta, Au) have significant absorption losses, especially for energies just above their absorption edges.

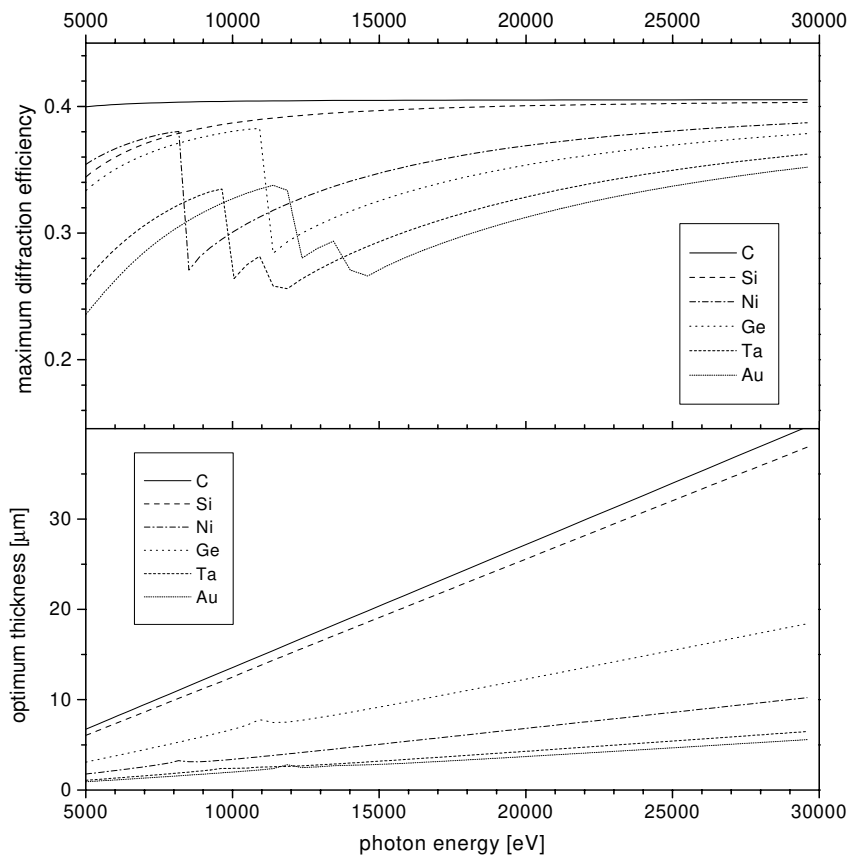


Figure 1: Maximum obtainable first order diffraction efficiency and optimum structure height of a binary diffractive optical element as a function of photon energy for a selection of elements.

The obtainable efficiency with light elements (C, Si) in this energy range is close to the theoretical limit of a pure phase grating of  $4/\pi^2 = 40.5\%$ . Unfortunately, for light materials, the required structure height to obtain a  $\pi$  phase shift is more than ten microns, which means enormous aspect ratios for sub-micron structure widths. The fabrication of nanostructures using standard technologies like reactive ion etching is limited to aspect ratios in the order of 10 due to limited control of the sidewall angles.

Wet etching of single crystal silicon offers a unique possibility for fabricating such very high aspect ratio structures. On Si substrates with  $\langle 110 \rangle$  orientation, lines along the  $\langle 112 \rangle$  direction have sidewalls with  $\langle 111 \rangle$  orientation. Therefore, an orientation-selective wet etch produces structures with vertical side walls<sup>16</sup>.

## 1- AND 2-DIMENSIONAL FOCUSING USING LINEAR FRESNEL ZONE PLATES

This method of anisotropic wet etching is obviously limited to producing linear diffractive structures and thus to one-dimensional focusing (see Figure 2A). To achieve two-dimensional focusing, we propose aligning two linear lenses with different focal lengths and orthogonal orientations along the optical axis as indicated in Figure 2C. Diffractive optical elements with linear structures leave an additional degree of freedom. By a tilt of  $\varphi$  around the axis perpendicular to the diffractive structures and the optical axis, the effective path through the structures can be increased by a factor of  $1/\cos \varphi$  (Figure 2 B,D).

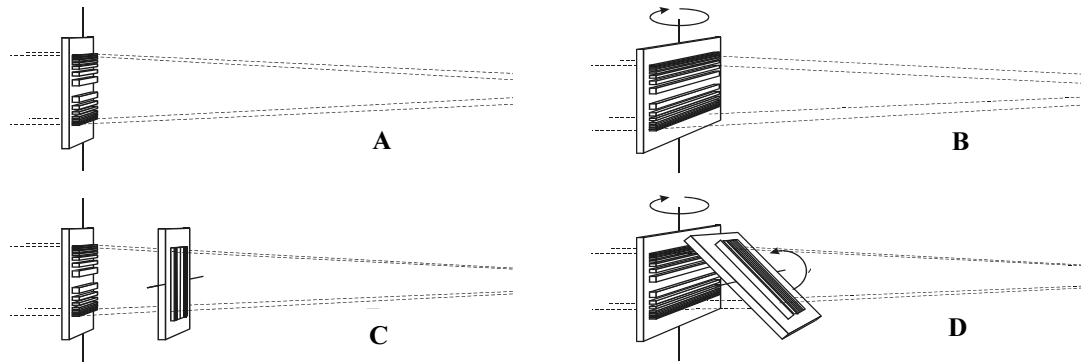


Figure 2: A linear zone plate can be used to produce a line focus (A). By tilting of the lenses, the effective path through the phase shifting structures can be varied (B, D.) in order to match the phase shift over a wide energy range and to increase the obtainable aspect ratio. A combination of two such devices will result in two-dimensional focusing (C, D).

In case of two perpendicular linear zone plates, the diffraction efficiencies of both devices  $\eta_1, \eta_2$  have to be multiplied to obtain the total efficiency  $\eta_{tot} = \eta_1 \eta_2$ . One might think that this is a major disadvantage over 2-dimensional microfocusing using a single (i.e. circular) zone plate. However, a closer look at a typical set-up on a hard x-ray insertion device beam line shows, that this is not necessarily the case. A zone plate (like all lenses) has to be coherently illuminated in order to give diffraction limited resolution. If the aperture of the zone plate is larger than the coherently illuminated area, the obtainable spot size will be limited to the size of the demagnified image of the source. Usually the spatial coherence of synchrotron sources is very different in the horizontal and vertical directions due to the asymmetry of the source size (see Figure 3). Let us consider a single lens with a round aperture. If the lens is small enough to be completely illuminated with coherent light, diffraction-limited focusing is possible in both horizontal and vertical directions, but only a small fraction of the coherent photons are actually collected (Figure 3 left). On the other hand, if the lens is made large enough to collect all coherent photons, a diffraction limited focusing is possible only in one direction (Figure 3 right).

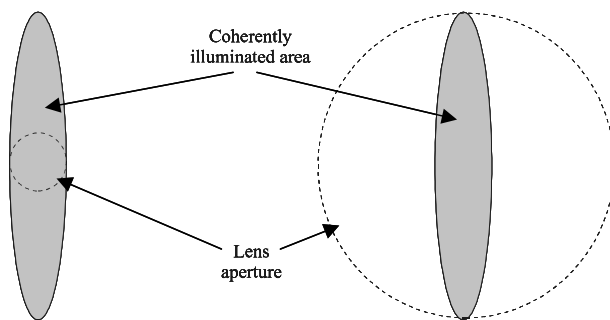


Figure 3: An elliptical source generates an elliptical region that is coherently illuminated (grey area). A lens with a circular aperture can either be small enough to be illuminated with coherent light (left), resulting in a loss of most coherent photons. A large lens aperture (right) collects all coherent photons, but loses its ability for diffraction limited focusing.

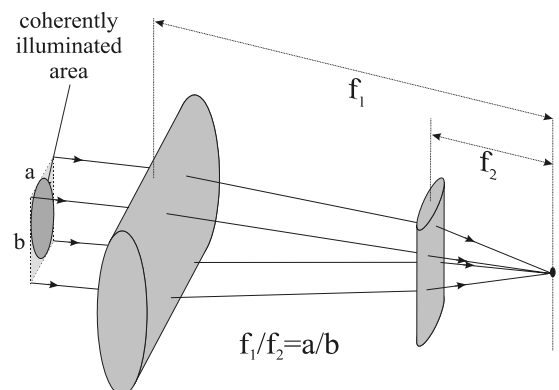


Figure 4: Coherence matched focusing by two linear lenses. All coherent photons are collected.

To match a microfocusing optic to the spatial coherence of an asymmetrical source, the horizontal and vertical focusing has to be performed by two separated optics similar to a Kirkpatrick-Baez mirror arrangement (Figure 4). By using two linear lenses with identical aperture angles but different focal lengths, all coherent photons can be focused into a diffraction limited, symmetrical spot. The ratio of the focal lengths should be identical to the source asymmetry  $a/b$ , i.e. the ratio of the source sizes in the horizontal and vertical directions. The flux compared to a single coherently illuminated lens with a spherical aperture (Figure 3 left) is also increased by this factor, when losses in the optical elements are ignored. In the case of two diffractive lenses, each with a diffraction efficiency  $\eta$ , the gain  $g$  in flux compared to a single circular lens with the same efficiency is  $g = \eta \cdot a/b$ . If, for example, the source is five times larger in the horizontal direction than it is in the vertical direction ( $a/b=5$ ), then  $g$  is larger than unity for  $\eta \geq 20\%$ . In this case, a set of two linear zone plates will deliver more flux into a diffraction limited spot than a single round zone plate with the same efficiency as one of the linear lenses. As will be presented in the next section, wet etched silicon linear lenses can be made with excellent efficiency for photon energies up to 29 keV.

## FABRICATION PROCESS

The lenses were made from  $\langle 110 \rangle$  oriented silicon wafers, 100 mm in diameter and 280  $\mu\text{m}$  thick according to the process steps depicted in figure 5. First, the unpolished side was coated with a 10  $\mu\text{m}$  thick layer of photo resist. An array of openings was defined by photo lithography and etched into the wafer by reactive ion etching in a  $\text{SF}_6$  plasma to form 50 - 60  $\mu\text{m}$  thick membranes (Figure 5a). Then, the polished side of the wafer was spin-coated with a 100 nm thick layer of polymethylmethacrylate (PMMA) electron-beam resist. The linear Fresnel zone plate patterns were defined by electron beam lithography (Figure 5b) and transferred into 30 nm thick chromium structures by a lift-off technique (Figure 5c). For extreme aspect ratios, the line patterns have to be aligned along the  $\langle 112 \rangle$  direction with an accuracy of better than  $0.1^\circ$  to avoid underetching of the Cr mask. In order to get at least one well-aligned lens per membrane a series of lenses were produced on each membrane. For each exposure the orientation differed by  $0.2^\circ$  from the previous one. Each line was generated by a single sweep of the electron beam, and the line width was varied by changing the defocus of electron beam according to a method described elsewhere in more detail<sup>17</sup>.

Before the wet etching process, the native oxide layer is removed by a 15 sec etch in 1:7 aqueous solution of buffered oxide etch (BOE). For the orientation selective etching of the silicon, we tried two different types of etching solutions : a) 100 ml ethylenediamine, 13 ml water, and 16 g pyrocatechol (EDP), b) a 20% aqueous solution of KOH. The etch speed for EDP at  $60^\circ\text{C}$  and for KOH at  $40^\circ\text{C}$  was 10  $\mu\text{m}/\text{h}$  for the  $\langle 110 \rangle$  direction and in the order of 0.1  $\mu\text{m}/\text{h}$  in the  $\langle 111 \rangle$  direction. Although the KOH solution gives more reproducible etch rates and is easier to handle, we found that it leads to much rougher surfaces (Figure 6) which may cause small-angle scattering of the incident x-rays. The Cr mask can be removed in an aqueous solution of potassiumhexacyanoferrate.

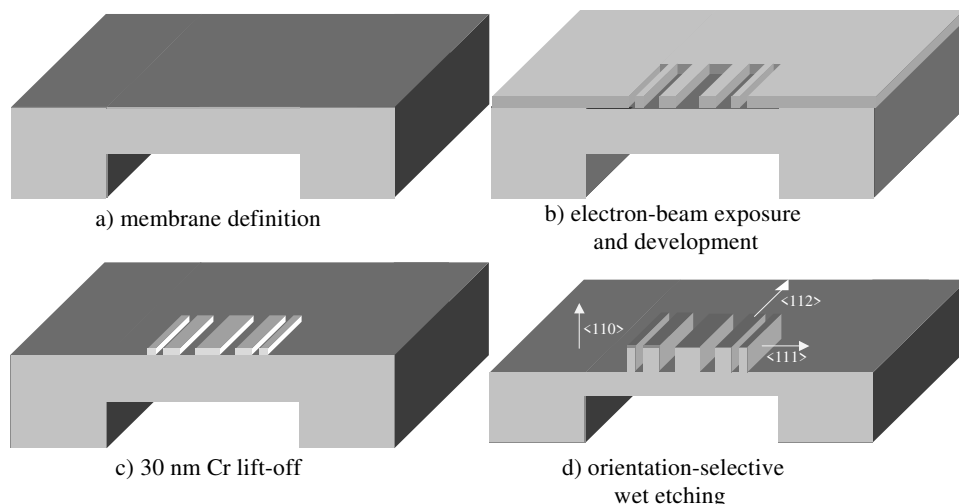


Figure 5: Schematic view of the fabrication process by electron-beam lithography, lift-off, and anisotropic wet etching

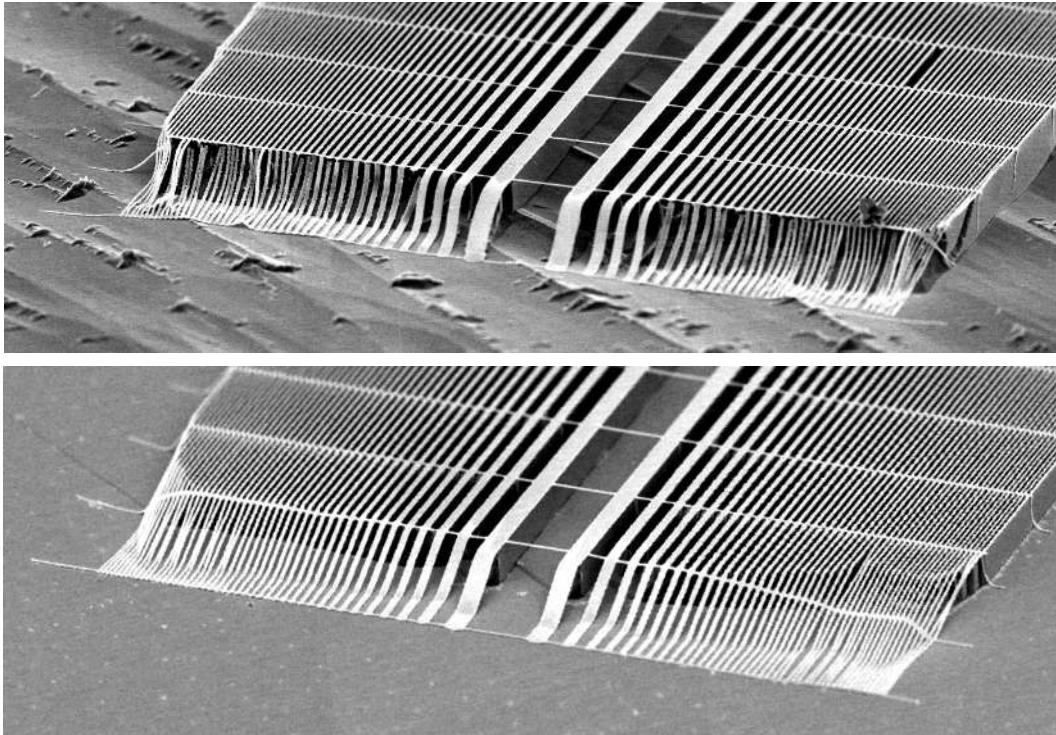


Figure 6: Wet etched linear zone plates with  $1\ \mu\text{m}$  high structures and  $100\ \text{nm}$  outermost zone width. The  $20\ \text{nm}$  thick  $\text{Cr}$  etch mask can be seen on top of the  $\text{Si}$  structures. Etching in a  $\text{KOH}$  solution (top image) results in a strong increase of the surface roughness compared to etching in an  $\text{EDP}$  solution (lower image).

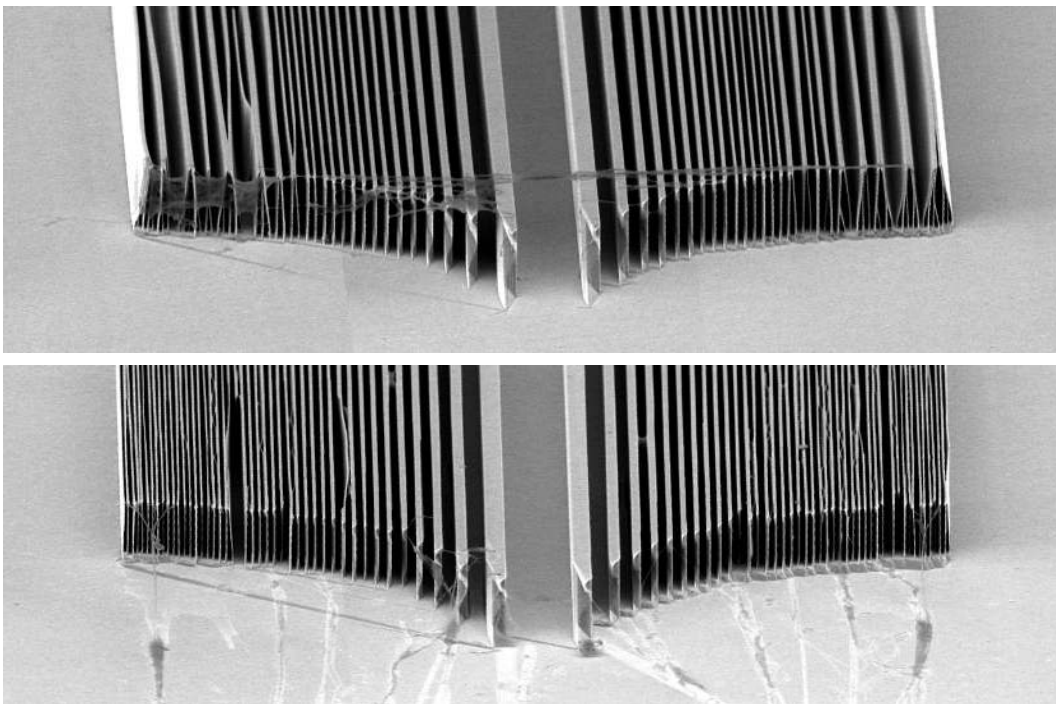


Figure 7: Linear zone plates with  $2.5\ \mu\text{m}$  high structures and  $100\ \text{nm}$  outermost zone width etched in  $\text{EDP}$ . The  $\text{Cr}$  etch mask has been almost completely removed. Drying in air leads to collapsing of structures with widths below  $200\ \text{nm}$  (top image) while critical point drying from liquid  $\text{CO}_2$  largely eliminates this problem (lower image).

The limited etch selectivity leads to a gradual narrowing of the etched lines, which has to be precompensated in the line widths defined by electron-beam lithography. This effect eventually limits the possible aspect ratio to about 50:1. Moreover, we encountered an additional limitation when the lenses were dried after the final rinsing step in high purity water: structures with aspect ratios above 25 tend to collapse due to capillary forces during the drying process<sup>18</sup>. Experiments applying a final rinsing step in a liquid with a lower surface tension (heptane) did not lead to any significant improvement. Better results were obtained by critical point drying in liquid CO<sub>2</sub> (figure 7) and freeze drying from cyclohexane. We fabricated various devices with structure widths down to 100 nm (half pitch). The obtained aspect ratios were in the region of 25 for 100 nm structures and up to 40 for 350 nm structures<sup>19</sup>.

## DIFFRACTION EFFICIENCY MEASUREMENTS

The diffraction efficiency of a Fresnel zone plate fabricated using the described technique with 5.5 μm high Si structures, an aperture of 200 μm, a length of 2.5 mm, an outermost zone width of 350 nm, and 5 μm support membrane thickness was measured at the BM5 bending magnet beam line of the European Synchrotron Radiation Facility (ESRF). The diffraction efficiency for the untilted lens is expected to be optimum at 4.9 keV photon energy. Due to the absorption of radiation by air, we were not able to measure the diffraction efficiency for energies below 8 keV. In addition we were restricted by the geometry of the Si <111> double crystal monochromator to values below 29 keV. The lens was mounted with the diffracting structures oriented horizontally, thus, focusing in the vertical direction. A slit with an opening of approximately 20 μm height and 200 μm width was scanned through the focal plane of the lens while recording the transmitted signal using a photo diode. The first order diffraction efficiency can be obtained by evaluating the integral over the focal peak. This method was previously developed to characterize Bragg-Fresnel lenses<sup>3</sup>. It has proven to be very accurate and robust, as it does not require exact knowledge of the slit dimensions.

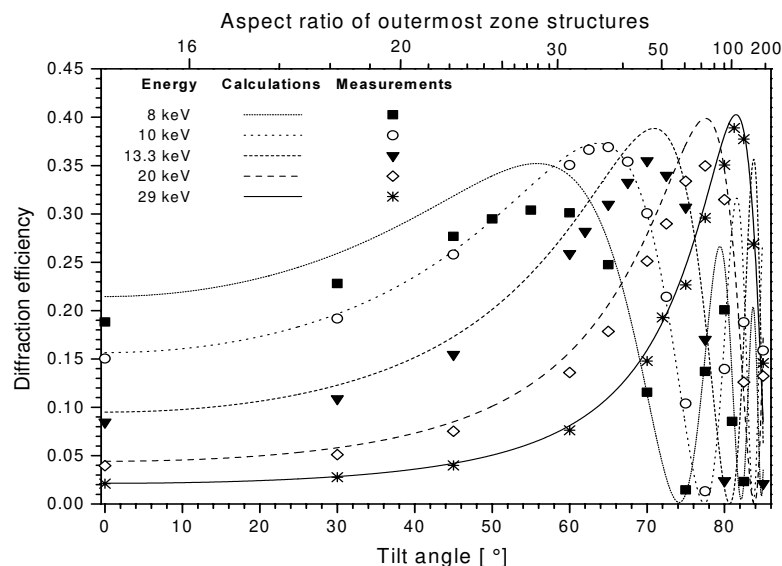


Figure 8: First order efficiency of a linear Fresnel zone plate with 5.5 μm high Si structures for photon energies between 8 keV and 29 keV as a function of the zone plate tilt angle. The lens aperture was 200 μm. The upper horizontal axis indicates the effective aspect ratio of the 350 nm wide outermost zones.

The calculated efficiency data and the measured values for 8, 10, 13.3, 20, and 29 keV photon energy are plotted in Figure 8. The curves reach their maxima at 55.8°, 63.6°, 70.9°, 77.5°, and 81.5° tilt angle, respectively, which corresponds to a phase shift of  $\pi$ . Oscillations at higher tilt angles with minima for values equivalent to even integers and maxima for odd multiples of  $\pi$  phase-shift can be observed. We were able to measure the diffraction efficiencies up to tilt angles of 85°, corresponding to an aspect ratio of 150. The measured data for 10 and 29 keV photon energy very closely follow the theoretical curves, whereas for the other energies, the measured data are somewhat lower than expected. This is probably due to a slight angular misalignment around the axis perpendicular to the optical axis and the tilt axis, which would mean a tilt of the structures sidewalls with respect to the beam. It should be noted, that this technique of increasing the effective aspect ratio by tilting can also be applied to zone plates with blazed zone profiles<sup>20, 21</sup> especially to enhance the diffraction efficiency for two-dimensional focusing by two linear lenses.

## SINGLE DIMENSION PARTIAL DECOHERER GRATINGS

The coherence of the wavefront generated by insertion devices of 3<sup>rd</sup> generation beam lines can be problematic in some applications. The imperfect optical elements (windows, mirrors, crystals and deposited particles) introduce phase perturbations on the wavefront, which induce intensity non-uniformity after beam propagation. Temporal fluctuations then result from the source spatial and angular variations as well as from optical elements vibrations. Although these “speckle like” phenomena are properly eliminated in imaging applications only by improving the quality of the optical elements, they also influence less demanding applications by degrading the quality of the normalization process. Creating a less coherent source in one dimension can therefore be very beneficial. Tuning the degree of partial coherence of the source by a pseudo-random diffruser oscillating at a rate much faster than the integration time of the detector has long been used in visible optics. Holographic diffusers or simply rotating ground glass have been used successfully. More recently, this technique has been used in the hard X-rays domain<sup>22</sup>. Although local feedback corrections on the source position have significantly improved the situation at a source like the ESRF, a partial decoherer with perfectly controlled parameters is still desirable.

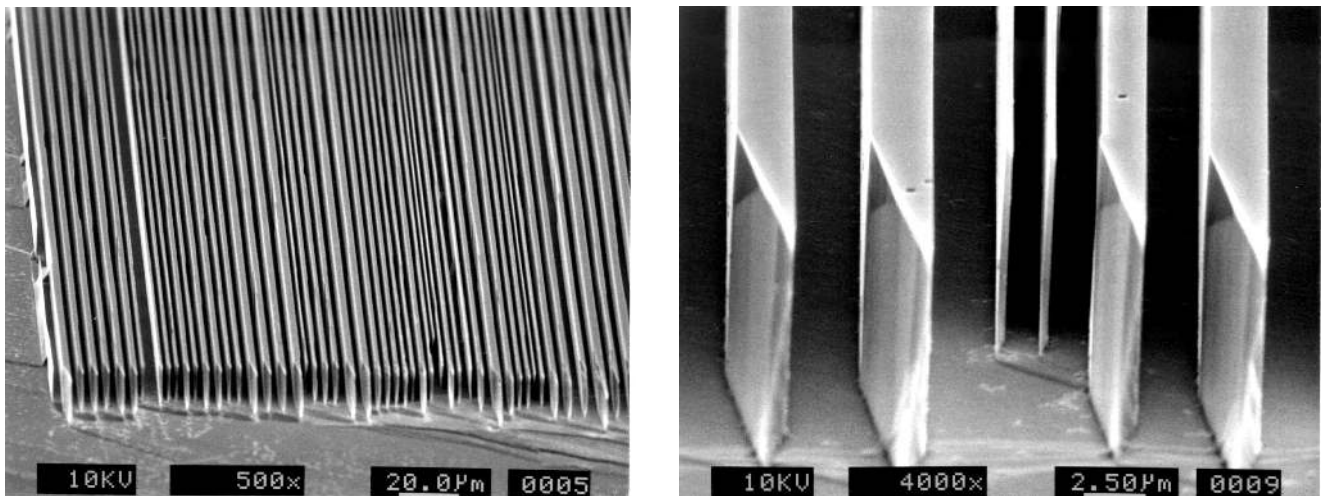


Figure 9: SEM images of a decoherer grating with pseudo-random pitch fabricated by wet etching of Si<110> substrates. The dimensions of the device are: width (perpendicular to lines) 1 mm, length (along lines): 4mm, structure height: 13  $\mu\text{m}$ , pitch range: 1.5 – 6.5  $\mu\text{m}$ , membrane thickness: approx. 5  $\mu\text{m}$ .

We pursue the approach to introduce a diffractive device into the beam consisting of a linear phase grating with pseudo random pitch. Figure 9 shows such a device fabricated from a single crystal <110> substrate by the described wet etching technique. The device has a weight of only 100 mg, so it can be easily vibrated with high frequencies without affecting the remaining set-up. The grating pitch covers a range of 1.5 – 6.5  $\mu\text{m}$ , resulting in a fan out of about 50  $\mu\text{rad}$  FWHM for 10 keV radiation. It is intended to be located at some meters from the sample, possibly in air, with vibration amplitude of only a few microns. The effect on the coherence properties depends on the actual distances between source and decoherer and between sample and decoherer, and can be chosen within certain limits. Similar to the linear zone plates, the device can be tuned over a wide range of photon energies by tilting. From the efficiency values close to the theoretical values obtained with the Fresnel zone plates it can be anticipated, that the zero order efficiency of the decoherer devices should be negligible. First experiments to test the decoherer devices at the ESRF are scheduled in the near future.

## BEAMSPLITTERS FOR X-RAY INTERFEROMETRY

The presented technique can of course also be applied for the fabrication of linear gratings with constant pitch. Because the phase shift introduced by the grating structures can be tuned to the optimum value of  $\pi$ , it can be expected that the zero order as well as higher diffraction orders will have small efficiencies compared to the first diffraction orders. Thus, such a device can be used as a hard x-ray beam splitter, as a planar wave incident on such a grating will be separated into two plane waves with equal intensity.

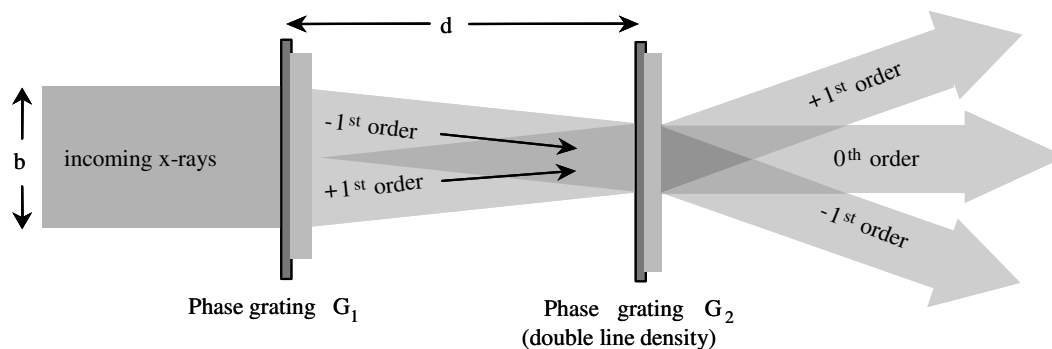


Figure 10: Schematic view of a shearing interferometer for hard x-rays consisting of two phase gratings.

For a grating pitch of several 100 nm, and wavelengths in the range of 0.1 nm, the angular separation of the two beams will be less than 1 mrad. Thus, this kind of beam splitter is not well suited for a Mach-Zehnder type of interferometer as introduced by Bonse and Hart<sup>23</sup>, which require a large angular separation of the two exit beams. However, these devices are suited to build a shearing interferometer as indicated in Figure 10. By superimposing two plane waves with a slight angular separation, deformations of the incident wave can be analyzed by evaluating the interference fringes using a second phase grating in the overlap region downstream of the beam splitter. Such a set-up could be used for wave front sensing, optics testing, or differential phase contrast imaging. The potential advantages over the Bonse-Hart type set-up are a larger spectral bandwidth and greatly reduced requirements with respect to the mechanical stability.

## SUMMARY AND OUTLOOK

The presented technology opens up a new way of fabricating diffractive optical elements for an energy range that was not accessible before. The method is most useful for obtaining devices to focus hard x-rays down to sub-micron spot sizes. The necessary technological steps to reach 100 nm spot sizes at 10 keV photon energy and above have been taken and the experimental verification of such a performance will be attempted in the near future.

The technique of tilting the diffractive devices with respect to the incident beam serves two purposes: firstly, it enables us to obtain effective aspect ratios of 100 or beyond, which makes it possible to use low absorbing materials such as silicon. Secondly, the phase shift introduced by the diffractive structures can be tuned over a wide energy range, making the diffractive optics versatile add-on devices in experimental set-ups. The tilting technique does not have to be used with structures fabricated by anisotropic wet etching, although this combination is particularly powerful due to its simplicity. The disadvantage of being limited to linear diffractive structures can be overcome by combining two devices with orthogonal orientations. It is shown that this does not necessarily result in a loss of total efficiency, when the asymmetry in the spatial coherence of the x-ray source is taken into account.

In contrast to refractive or reflective optical components, diffractive optics can be made with sufficient precision using standard lithography equipment, to preserve the coherence of the incident radiation. For focusing devices this means that the spatial resolution is not limited by aberrations but only by diffraction on the optics aperture. Furthermore, a variety of other applications such as interferometry can be addressed.

## ACKNOWLEDGMENTS

We would like to thank B. Haas and S. Blunier for their assistance in fabricating the Si<110> membranes. M. Müller and A. Grubelnik are acknowledged for providing the advanced drying processes. We are also indebted to J. Hozowska for her help during the efficiency measurements at the ESRF. This work was partially funded by the Swiss National Science Foundation.



## REFERENCES

1. E. Ziegler, O. Hignette, Ch. Morawe, R. Tucoulou: submitted to Nucl. Instrum. Methods A (2000)
2. S.M. Kuznetsov, I. Snigireva, A. Snigirev, P. Engstrom, and C. Riekel: Appl. Phys. Lett. **65** (1994) 827 - 829
3. C. David, A. Souvorov: Rev. Sci. Instr., Vol. 70, no. 11 (1999) 4168 - 4173
4. T. Tomie: Japanese Patent No. 06045288 (1994), US Patent No. 5594773 (1997), German Patent No. DE1995019505433 (1998)
5. A. Snigirev, V. Kohn, I. Snigireva, B. Lengeler: Nature **384** (1996) 49 - 51
6. B. Lengeler, C. Schroer, J. Tümmeler, B. Benner, M. Richwin, A. Snigirev, I. Snigireva and M. Drakopoulos: J. Synchrotron Rad. **6** (1999) 1153 - 1167
7. E. Anderson and D. Kern, in: X-Ray Microscopy III, Eds.: A.G. Michette, G.R. Morrison, and C.J. Buckley, Springer (1990) 75
8. D. Weiss, M. Peuker, and G. Schneider, Appl. Phys. Lett. **72** (1998) 1805 - 1807
9. G. Schneider, T. Schliebe, and H. Aschoff, J. Vac. Sci. Technol. **B 13** (1995) 2809 - 2811
10. S.J. Spector, C.J. Jacobsen, and D.M. Tennant, J. Vac. Sci. Technol. **B 15** (1997) 2872 - 2875
11. C. David, B. Kaulich, R. Medenwaldt, M. Hettwer, N. Fay, M. Diehl, J. Thieme and G. Schmahl: J. Vac. Sci. Technol. **B 13** (1995) 2762-2766
12. W. Yun, B. Lai, Z. Cai, J. Maser, D. Legnini, E. Gluskin, Z. Chen, A.A. Krasnoperova, Y. Vladimirovsky, F. Cerrina, E. Di Fabrizio, M. Gentili, Rev. Sci. Instrum. **70** (1999) 2238-2241
13. see for example: J. Baruchel, P. Cloetens, J. Härtwig, W. Ludwig, L. Mancini, P. Pernot, M. Schlenker: J. Synchrotron Rad. **7** (2000) 196 - 201
14. J. Kirz, J. Opt. Soc. Am. **1** (1974) 301 - 309
15. B.L. Henke, E.M. Gullikson, and J.C. Davis: Atomic Data and Nuclear Data Tables **54** (1993) 181-342
16. For a review of vertical silicon wet etching see: D.L. Kendall: J. Vac. Sci. Technol. A **8** (1990) 3598 - 3605
17. C. David and D. Hambach: Microelectronic Engineering **46** (1999) 219 - 222
18. C. David, E. Ziegler, B. Nöhammer, J. Synchrotron Rad. **8** (2001) 1054 - 1055
19. C. David, B. Nöhammer, E. Ziegler, Appl. Phys. Lett., accepted for publication
20. E. Di Fabrizio, F. Romanato, M. Gentili, S. Cabrini, B. Kaulich, J. Susini, R. Barrett: Nature, **401** (1999) 895 - 897
21. C. David: Microelectronic Engineering **53** (2000) 677 - 680
22. P. Cloetens, R. Barrett, J. Baruchel, J.P. Guigay, M. Schlenker: J. Phys. D: Appl. Phys., **29** (1996) 133-146
23. U. Bonse, M. Hart: Appl. Phys. Lett. **6** (1965) 155 - 156